Part One Structure and Bonding

1
Bonding in Coordination Compounds

1.1
d Wavefunctions

The wavefunction of an electron, in polar coordinates (Figure 1.1), is expressed by the formula $\phi_{n,l,m} = R(r)_{n,l}Y(\theta,\phi)_l^m$, where $R_{n,l}$ is the radial part and Y_l^m the angular part. Symmetry operations only alter the angular part, regardless of the value of n (the principal quantum number).

Y_l^m corresponds to what are known as spherical harmonics, which can be broken down into two independent parts, Θ_l^m and Φ_m, which in turn depend on the angles θ and ϕ of the polar coordinates, $Y_l^m = \Theta_l^m\Phi_m$. Φ_l^m are the standard Legendre polynomials, which depend on $\sin\theta$ and $\cos\theta$; and $\Phi_m = (2\pi)^{-1/2}e^{im\phi}$.

The wavefunctions of the orbitals s, p, d and f are expressed as follows: Y_0^0 refers to an s orbital; Y_1^0, Y_1^1, Y_1^{-1} to the three p orbitals; Y_2^0, $Y_2^{\pm1}$, $Y_2^{\pm2}$ to the d orbitals; and Y_3^0, $Y_3^{\pm1}$, $Y_3^{\pm2}$, $Y_3^{\pm3}$ to the f orbitals. The mathematical expressions of these functions have an imaginary part, $\Phi_m = (2\pi)^{-1/2}e^{im\phi}$. Given that $e^{\pm im\phi} = \cos(m_l\phi) \pm i\sin(m_l\phi)$, one usually works with linear combinations of the orbitals, which enable the imaginary part to be suppressed. Those functions in which the imaginary part has been suppressed are known as *real wavefunctions* of the atomic orbitals. Using the mathematical expressions that relate the polar to the Cartesian coordinates ($r^2 = x^2 + y^2 + z^2$; $x = r\sin\theta\cos\phi$; $y = r\sin\theta\sin\phi$; $z = r\cos\theta$) it is possible to determine the equivalence between the real wavefunctions in polar and Cartesian coordinates, which are those conventionally used to 'label' the d orbitals (xz, yz, xy, x^2-y^2, z^2) (Table 1.1).

1.2
Crystal Field Effect on Wavefunctions

1.2.1
Qualitative Aspects

In 1930 Bethe and Van Vleck studied the effect of isolating a Na^+ cation by placing it inside an ionic lattice, such as NaCl. They sought to determine what happens

Coordination Chemistry. Joan Ribas Gispert
Copyright © 2008 WILEY-VCH Verlag GmbH & Co. KGaA, Weinheim
ISBN: 978-3-527-31802-5

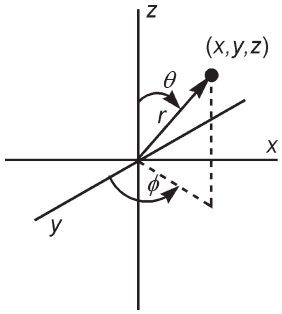

Figure 1.1 Relationship between cartesian and polar coordinates.

Table 1.1 Imaginary and *real* angular wavefunctions of d orbitals [1, 2].

Y_2^m	*Imaginary function*	*Real function (combination)*	*Real function*		*Real function*[a]	*Orbital*
			Normalizing factor	*Angular function*		
Y_2^0	$(5/8)^{1/2}(3\cos^2\theta - 1)(2\pi)^{-1/2}$	$\|0\rangle$	$(\sqrt{5}/\pi)/4$	$(3\cos^2\theta - 1)$	$2z^2 - x^2 - y^2$	d_{z2}
Y_2^1	$(15/4)^{1/2}\sin\theta\cos\theta\,(2\pi)^{-1/2}\,e^{+i\phi}$	$2^{-1/2}[\|1\rangle + \|-1\rangle]$	$(\sqrt{15}/\pi)/2$	$\sin\theta\cos\theta\cos\phi$	xz	d_{xz}
Y_2^{-1}	$(15/4)^{1/2}\sin\theta\cos\theta\,(2\pi)^{-1/2}\,e^{-i\phi}$	$2^{-1/2}[\|1\rangle - \|-1\rangle]$	$(\sqrt{15}/\pi)/2$	$\sin\theta\cos\theta\sin\phi$	yz	d_{yz}
Y_2^2	$(15/16)^{1/2}\sin^2\theta\,(2\pi)^{-1/2}\,e^{+2i\phi}$	$2^{-1/2}[\|2\rangle + \|-2\rangle]$	$(\sqrt{15}/\pi)/4$	$\sin^2\theta\cos2\phi$	$x^2 - y^2$	$d_{x^2-y^2}$
Y_2^{-2}	$(15/16)^{1/2}\sin^2\theta\,(2\pi)^{-1/2}\,e^{-2i\phi}$	$2^{-1/2}[\|2\rangle - \|-2\rangle]$	$(\sqrt{15}/\pi)/4$	$\sin^2\theta\sin2\phi$	xy	d_{xy}

a Cartesian coordinates.

to the energy levels of the free ion when it is placed inside the electrostatic field, known as the *crystal field*, which exists in the crystal. It was known that, prior to being subjected to the crystal field, the energy levels of the free ion are degenerate. They demonstrated that, depending on the symmetry of the crystal field, this degeneracy is lost; at the same time they developed a theory which they applied to 3D ionic solids. However, 20 years were to pass before chemists applied the theory to coordination compounds. The essential idea of the model applied to complexes is to assume that the coordination sphere of the anions or ligands surrounding a metal ion behave as a set of negative point charges which interact repulsively with respect to the electrons of the central metal cation. The two single electrons of a ligand act like a negative point charge (or like the partial negative charge of an electric dipole), which undergoes a repulsive effect with respect to the electrons of the d orbitals of the central metal ion. The theory is very simple, easy to visualize and correctly identifies the importance of the symmetry of the orbitals. The bond is thus essentially electrostatic: there is cation(+)/ligand(−) attraction but, at

the same time, repulsion between the ligands and the electrons of the central cation.

In this first chapter, the theory will only be used to explain the bonding in coordination compounds. The concept of term, multiplet, state, etc. will be dealt with in Chapter 8. Group theory is of great use in both situations.

Starting from a cyclic point group it is possible to obtain the irreducible representations for any value of the quantum number l, by means of the following formula:

$$\chi(\alpha) = \left[\sin\left(l + \frac{1}{2}\right)\alpha\right] / \sin(\alpha/2) \tag{1}$$

(α = angle of rotation corresponding to the cyclic group; $\alpha \neq 0$)

This formula can be used to calculate the *qualitative* splitting of the atomic orbitals for any crystal field of a given symmetry (Tables 1.2 and 1.3).

It can be seen that the p orbitals do not split under the effects of octahedral or tetrahedral fields. However, if the symmetry is reduced they do split. Obviously, the s orbital never splits, regardless of the symmetry.

For the two main symmetries (O_h and T_d) the splitting caused by the crystal field can be visualized intuitively by drawing the d orbitals together with the ligands. Figure 1.2 illustrates the splitting of d orbitals for octahedral symmetry, while Figure 1.3 does the same for tetrahedral symmetry.

In an octahedral complex (O_h) the six ligands are situated along cartesian axes (Figure 1.2) whose origin is the metal ion. Therefore, the ligands are close to the

Table 1.2 Splitting of the atomic orbitals in O_h symmetry.

Orbital	l	$\chi(E)$	$\chi(C_2)$	$\chi(C_3)$	$\chi(C_4)$	*Irreducible representation*
s	0	1	1	1	1	a_{1g}
p	1	3	–1	0	1	t_{1u}
d	2	5	1	–1	–1	$e_g + t_{2g}$
f	3	7	–1	1	–1	$a_{2u} + t_{1u} + t_{2u}$

Table 1.3 Splitting of the orbitals in T_d, D_{4h}, D_3 and D_{2d} symmetry fields.

	T_d	D_{4h}	D_3	D_{2d}
s	a_1	a_{1g}	a_1	a_1
p	t_2	$a_{2u} + e_u$	$a_2 + e$	$b_2 + e$
d	$t_2 + e$	$a_{1g} + b_{1g} + b_{2g} + e_g$	$a_1 + 2e$	$a_1 + b_1 + b_2 + e$
f	$a_2 + t_2 + t_1$	$a_{2u} + b_{1u} + b_{2u} + 2e_u$	$a_1 + 2a_2 + 2e$	$a_1 + a_2 + b_2 + 2e$

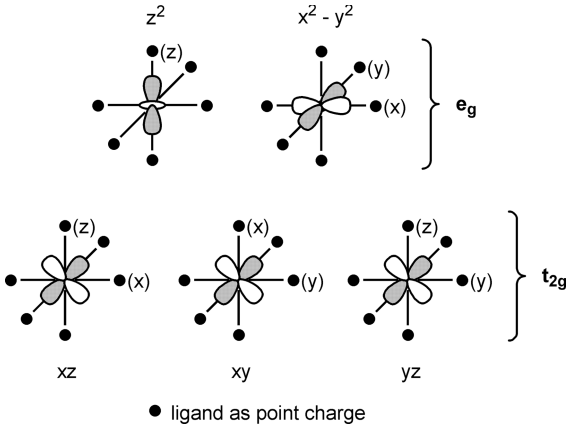

Figure 1.2 Representation of the d orbitals and point charges in an O_h crystal field.

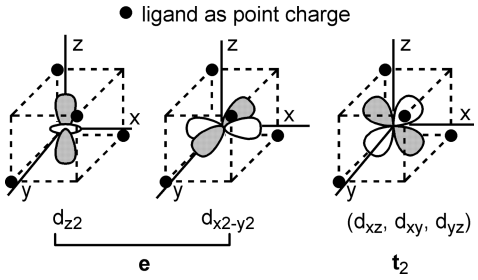

Figure 1.3 Representation of the d orbitals and point charges in a T_d crystal field.

d_{z2} and d_{x2-y2} orbitals, whose symmetry label is e_g. The other three d orbitals (d_{xy}, d_{xz}, d_{yz}) are further away from the ligands. Their symmetry label is t_{2g}. If we consider the repulsions between the d orbitals and the ligand electrons, it is logical to assume that these repulsions are greater between the ligands and the e_g orbitals than between the same ligands and the t_{2g} orbitals (which are directed toward the bisectors of the planes *xy, xz, yz*). Therefore, a simple logical deduction tells us that the five d orbitals have split into two groups: e_g and t_{2g}. This same logic enables us to deduce that the potential energy of the three degenerate t_{2g} orbitals is less than the energy of the two degenerate e_g orbitals.

A tetrahedral field also splits the five d orbitals into two sets, t_2 (d_{xy}, d_{xz}, d_{yz}) and e (d_{z2} and d_{x2-y2}). It can easily be seen that the splitting of the d orbitals must be less than and the reverse of what occurs in the octahedral case. Indeed, with tetrahedral geometry none of the ligands moves toward the central ion according to the direction of the orbitals. In this case the t_2 orbitals are closer to the ligands, as they are directed toward the mid-point of the edges, whereas the e orbitals are directed towards the center of the faces (Figure 1.3).

1.2.2 Quantitative Aspects

Group theory does not tell us anything about the relative energies of the different groups of orbitals. In order to determine the corresponding energies it is necessary to use energy calculations with the corresponding operators.

1.2.2.1 Energy Operator of the Ligand Field

The potential created by six point charges (assuming O_h geometry) at a point x,y,z is:

$$V_{(x,y,z)} = \sum_{i=1}^{6} ez_1 / r_{ij}$$

where r_{ij} is the distance from the charge i to the point x,y,z. $1/r_{ij}$ can be written according to the abovementioned spherical harmonics.

1.2.2.2 Effect of V_{oct} on d Functions

The energy calculation is complicated and beyond the scope of this book. Further information can be found in specialized books, such as that of Figgis and Hitchman [1]. The final result for the energy involved in splitting the d orbitals is $10Dq$, where $D = 35ze/4a^5$ and $q = 2e\langle r\rangle^4/105$. Therefore, $Dq = (1/6)(ze^2\langle r\rangle^4/a^5)$. If point charges representing the ligand atoms are replaced by point dipoles, which provides a more realistic representation of ligands such as water or ammonia, a similar expression for Dq is obtained: $Dq = 5\mu\langle r\rangle^4/6a^6$. In both expressions ze is the charge of the anion, a is the internuclear distance between the metal and the anion or dipole and $\langle r\rangle$ is the average distance of the d orbital electron from its nucleus.

The splitting of the d orbitals, with their corresponding energies, is shown in Figure 1.4. Although the functions |1> (xz) and |–1> (yz) have been written separately, they can be combined linearly. Any linear combination is permitted, as in a cubic field they are degenerate functions. The linear combinations of |2> and

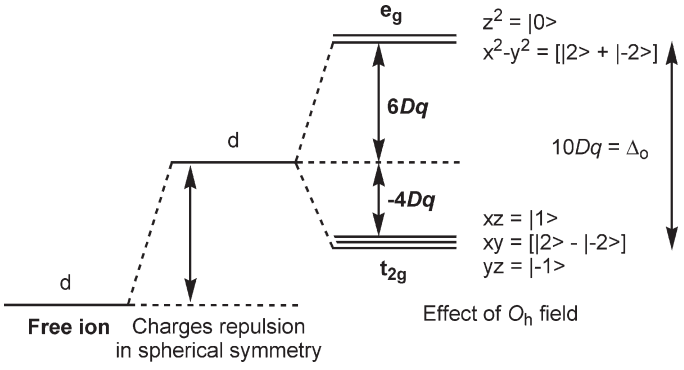

Figure 1.4 Splitting of the d orbitals in a crystal field of O_h symmetry.

$|-2>$ are *necessary* because the corresponding orbitals belong to different symmetries. They cannot be indicated as $|2>$ and $|-2>$.

The energy difference $10Dq = \Delta_o$ is termed the *crystal field splitting parameter*. The fact that there are only two types of orbitals (e_g and t_{2g}) means that if the separation between them is $10Dq$, the energy of the t_{2g} orbitals will be $-4Dq$ and that of the e_g orbitals $6Dq$, in order to fulfil the principle of energy conservation.

1.2.2.3 Crystal Field Splitting Parameter

The parameter $10Dq$ varies according to the identity of the ligands and the central ion. On the basis of many empirical observations, ligands can be grouped into what is known as the *spectrochemical series* according to the intensity of the crystal field they create, from lesser to greater energy. As regards some of the main ligands, the order of the spectrochemical series is:

$$I^- < Br^- < S^{2-} < SCN^- < Cl^- < NO_3^- < N_3^-, F^- < OH^- < ox < O^{2-} < H_2O < NCS^-$$
$$< CH_3CN < NH_3 \approx py < en < bpy < phen < NO_2^- < PPh_3 < CN^- < CO$$

From the point of view of crystal field theory, the relationship $F^- > Cl^- > Br^- > I^-$ is logical, as the smallest anion has more repulsion energy (q_1q_2/r) with decreasing r. However, crystal field theory cannot explain why an anionic ligand such as OH^- creates a weaker field than H_2O, or why CN^- and CO are among the ligands with the strongest field. This is one of the theory's weak points, and the explanation for it is to be found in the theory of molecular orbitals.

The values of $10Dq$ also depend on the metal ion. In general, the most important variations are as follows:

- $10Dq$ increases with the oxidation number. For example, for the divalent ions of the first transition series the value of Dq varies between 700 and 3000 cm^{-1}, whereas for trivalent ions it varies between 1200 and 3500 cm^{-1}.
- $10Dq$ increases upon moving down a group. If, for an M^{3+} ion of the first transition series, Dq has a value of 1200–3500 cm^{-1}, then the value for the second and third series will be 2000–4000 cm^{-1}. In general, the value of $10Dq$ increases by 50% when moving from the first to the second transition series, and by 25% when passing from the second to the third series.

On the basis of a wide variety of experimental data, it is possible to calculate empirically the value of $10Dq$, as the part corresponding to the metal and the part corresponding to the ligand can be parametrized: $10Dq = M\Sigma n_i L_i \times 10^3$ (cm^{-1}) [3, 4].

1.2.2.4 Weak and Strong Fields. Crystal Field Stabilization Energy

Placing one, two or three electrons in the d orbitals of an octahedral complex does not present a problem, as their placement is necessary $(t_{2g})^1$, $(t_{2g})^2$ and $(t_{2g})^3$. The problem arises when we want to place a fourth electron (or more). The new elec-

tron may be placed in two different sites: it may remain in the t_{2g} orbitals and pair with an existing electron, which results in energy destabilization due to the pairing energy of the electrons, *P*; alternatively, it may jump to the (free) e_g orbitals, and thus it will not have to pair, although it will have to overcome the positive energy $10Dq$. Naturally, which of the two phenomena occurs will depend on the *relative* values of $10Dq$ and *P*. If $10Dq >> P$ the electrons will tend to be paired in the t_{2g} orbitals; if $10Dq << P$ the electrons will tend to jump to the e_g orbitals. The former case is known as *strong field* or *low spin*, whereas the latter is referred to as *weak field* or *high spin*. This situation occurs for d^4, d^5, d^6 and d^7 configurations. The electron configurations d^8, d^9 and d^{10} only have one possibility, as is the case for d^1, d^2 and d^3.

Figure 1.5 illustrates these possibilities for all configurations. For each one of the configurations the figure in brackets is what is termed the *crystal field stabilization energy* (CFSE). It can be calculated by multiplying the number of electrons in the t_{2g} orbitals by $-4Dq$ and the number of electrons in the e_g orbitals by $6Dq$. The pairing energy, *P*, is always positive. The final energy calculation will be given by

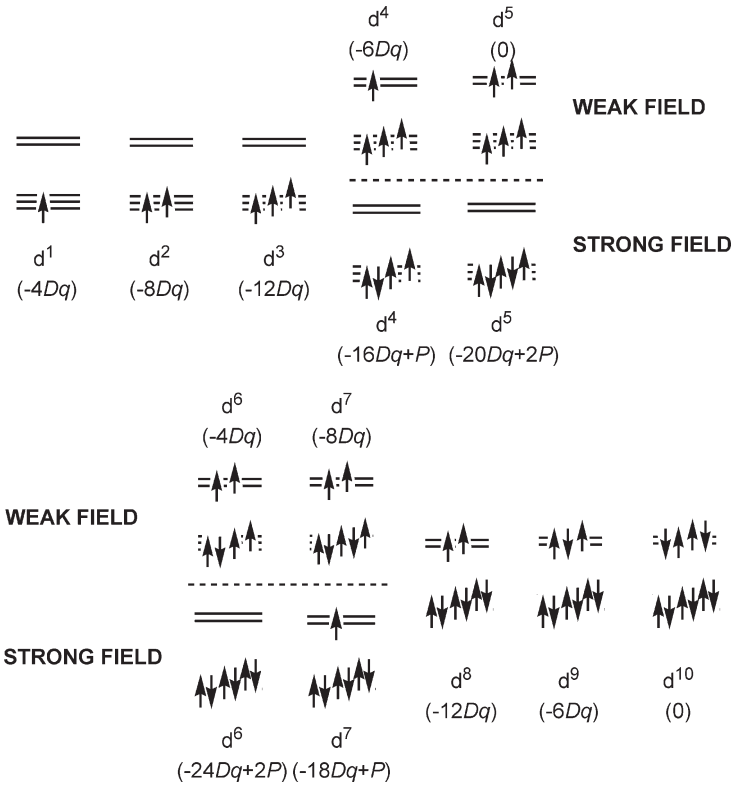

Figure 1.5 d-orbital occupancy in a crystal field of O_h symmetry (for both weak and strong field).

adding the value of P as many times as there are numbers of electron pairs in the configuration. There is one important detail to bear in mind here: if, in the four configurations in which a strong or weak field is possible, the energies of the two fields are mathematically equal, the two configurations will be in equilibrium. Any small external perturbation (temperature, pressure, etc.) may easily result in a switch from one configuration to the other. This phenomenon, known as *spin transition*, is of great importance when studying the magnetism of this series of complexes.

Remark: for the calculation of the pairing repulsion energy it is necessary to take into account the pairing energy in the spherical shell, before the application of the crystal field [5]. For $d^6 = P$; $d^7 = 2P$; $d^8 = 3P$; $d^9 = 4P$ and $d^{10} = 5P$.

All the above is valid for elements of the first transition series. Complexes of the second and third series generally adopt the low spin (strong field) configuration because, even with ligands that create a weak field, the field produced by the ion is sufficiently intense.

1.2.2.5 Splitting of d Orbitals in a Tetrahedral Field

$V_{tet} = -(4/9)\,V_{oct}$, and therefore $Dq_{tet} = -(4/9)\,Dq_{oct}$. This relationship can be verified by means of the angular overlap model of molecular orbital theory (see below). As a consequence, tetrahedral complexes are exclusively weak field complexes and there is no need to distinguish between two types, as in the case of octahedral complexes.

1.2.2.6 Splitting of d Orbitals in a Tetragonally-distorted Octahedral Field. Square-planar Complexes

According to group theory, when a crystal field of D_{4h} symmetry is applied, the d orbitals split into $a_{1g}(z^2) + b_{1g}(x^2 - y^2) + b_{2g}(xy) + e_g(xz, yz)$ (Table 1.3). Let us begin by studying the effect of a tetragonal distortion on the relative energies of the t_{2g} and e_g orbitals of a complex with O_h symmetry. From the point of view of group theory, the new point group will be D_{4h}, regardless of whether the distortion takes the elongated or compressed form. An elongation with respect to the z axis will result in the stabilization of all the orbitals with a z component, as the increasing distance between the two ligands will lead to lower ligand–electron repulsion energy. In contrast, in the case of compression the energy diagram will be the other way round: the orbitals with a z component will become more unstable due to greater repulsion. These effects are shown, for both cases, in Figure 1.6.

If the distortion in the form of elongation is large enough the two ligands will separate in the *trans conformation*, giving rise to a square-planar complex (D_{4h}). Figure 1.6B shows the energy diagrams, starting from an elongated octahedral complex. It is demonstrated that $\Delta_{sp} \approx 1.3\Delta_o$.

Although the same reasoning can be applied to other geometries it is generally the case, except for octahedral, tetrahedral and square-planar geometry, that molecular orbital theory offers a much more realistic approach. Even in the case of the above-mentioned complexes, crystal field theory ignores what are properly covalent

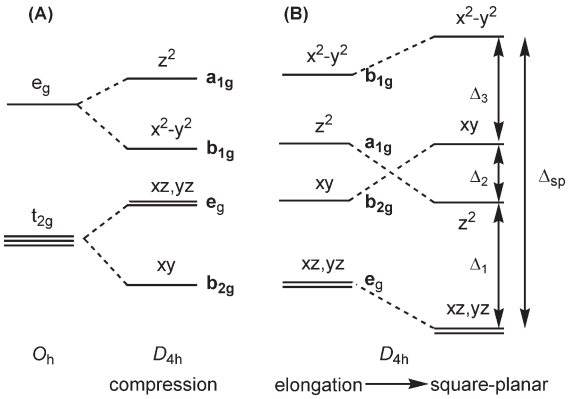

Figure 1.6 Compression or elongation of an O_h crystal field. Extrapolation to a square-planar geometry.

bond interactions between the metal ion and the ligands, and thus it tends to be replaced by *ligand field theory* (see Chapter 8).

1.3 Molecular Orbital Theory

As for non-coordination compounds, two theories can be applied to explain covalency: valence bond theory and molecular orbital theory. In the first the electrons are assumed to be localized: it is thus easy to explain the geometry, and it is necessary to introduce the 'artificial' concept of *hybrid* orbitals. In all books on General and Inorganic Chemistry, the valence bond theory applied to complexes with the typical hybridizations sp^3, sp^3d, sp^3d^2 etc. is explained, with more or less detail, emphasizing its current limitations. Thus, the interested reader can consult any of these books. Anyway, this concept of hybridization in coordination compounds has undergone a 'renaissance' since the Hoffmann definition of the '*isolobal analogy*' concept, which will be treated in Chapter 6.

In molecular orbital (MO) theory it is assumed that the bond between the central ion and the ligands is essentially covalent, and produced by the overlap of the s, p, and d orbitals of the central ion and the ligand group orbitals of adequate symmetry.

In this approach it is necessary to distinguish between qualitative aspects (symmetry of the MOs formed) and quantitative ones (energy of the MOs). With regard to the qualitative aspects it is once again necessary to turn to group theory, and there is really no difference between determining the nature and symmetry of the molecular orbitals of a simple molecule such as water and those of a coordination compound. The only difference lies in the fact that in a complex the d orbitals *necessarily* play a role, as they are the most important in this type of molecule.

As clearly indicated by Y. Jean in his recent book [6], there are four stages to the general procedure for constructing the MOs of an ML_n complex: (i) find the appropriate point group symmetry; (ii) determine the symmetry properties of the orbitals of the central metal atom (character tables); (iii) do not consider the ligand orbitals individually, but use linear combinations of these orbitals adapted to the symmetry of the complex: symmetry-adapted orbitals [or symmetry-adapted linear combinations (SALCs)]; (iv) allow metal and ligand orbitals to interact. Only orbitals of the same symmetry can interact, since their overlap is not zero.

Tables 1.2 and 1.3 show the symmetry labels of the s, p and d orbitals for O_h, T_d and other geometries. All that is required, therefore, is to construct the ligand group orbitals (by means of their projection operators) and combine them adequately with the orbitals of the central ion. Obviously, this approach will be valid for both σ and π bonds. Two conditions must be met with these ligand orbitals: they must be close in energy to those of the metal, and their overlap must also be substantial.

In order to calculate the energies it is necessary to turn to quantum methods, which may be very simple or extraordinarily complicated. The simplest method is what is known as the Angular Overlap Model; this will be discussed below and offers solutions to the energy calculations which are accurate enough for the objectives set within this book. Another more sophisticated method is the extended-Hückel model, which can be applied using a PC and the now widely available software program CACAO (**c**omputer **a**ided **c**omposition of **a**tomic **o**rbitals) [7]. Other increasingly sophisticated methods require significant calculation times. These methods will not be discussed in this chapter.

1.3.1
Molecular Orbitals of an Octahedral Complex

1.3.1.1 σ Molecular Orbitals

The symmetry labels of the s, p, and d orbitals are known (Table 1.2), so all that is required is to calculate the group orbitals on the basis of the ligand orbitals which can be adequately combined. There are several ways of representing the ligand orbital that is involved in the σ interaction: as an s orbital, as a p orbital, or as a hybrid (s–p) orbital directed toward the metallic center (Figure 1.7). It should be borne in mind that the order of the six orbitals in Figure 1.7 is totally arbitrary, as is the choice of the coordinate axes.

In the O_h point group the six σ orbitals of the ligands can be grouped according to the symmetry group orbitals $a_{1g} + e_g + t_{1u}$ (readers can easily verify this). By applying the projection operators we obtain the group orbitals as combinations of these six orbitals, and their adaptation to the symmetry of the central ion orbitals can be correlated. This calculation is rarely made in any book on Group Theory. Due to the high symmetry of an octahedral complex the group orbitals can be derived by simple intuition, and represented as in Figure 1.8, without needing to resort to projection operators. These results are given in Table 1.4 and Figure 1.8.

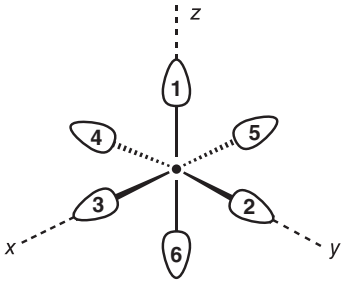

Figure 1.7 Ligand orbitals (σ character) in an octahedral complex.

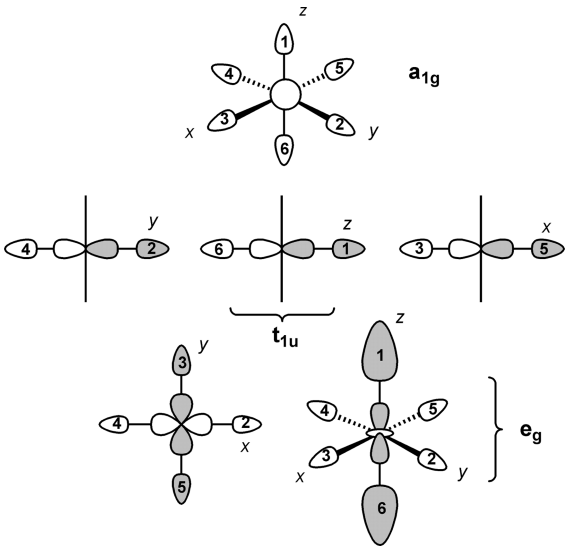

Figure 1.8 Ligand group orbitals and the corresponding metal ion orbitals, with their symmetry label (σ-bond; O_h symmetry).

Table 1.4 Correlation between ligand group orbitals and those of the central ion (O_h).

Metal orbital	*Symmetry*	*Ligand group orbitals*
s	a_{1g}	$\sigma_1 + \sigma_2 + \sigma_3 + \sigma_4 + \sigma_5 + \sigma_6$
p_z	t_{1u}	$\sigma_1 - \sigma_6$
p_x		$\sigma_3 - \sigma_5$
p_y		$\sigma_2 - \sigma_4$
d_{z2}	e_g	$2\sigma_1 + 2\sigma_6 - \sigma_2 - \sigma_3 - \sigma_4 - \sigma_5$
d_{x2-y2}		$\sigma_2 - \sigma_3 + \sigma_4 - \sigma_5$
$d_{xy,\ xz,\ yz}$	t_{2g}	–

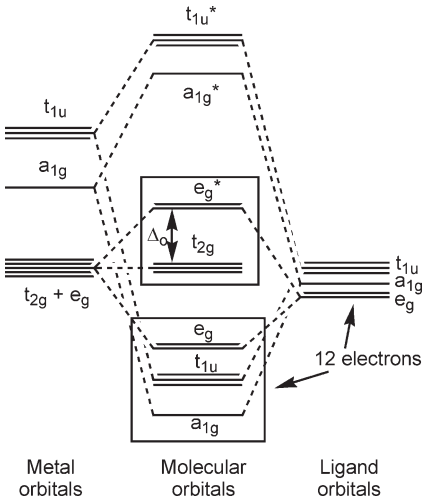

Figure 1.9 MO diagram (only σ orbitals) for an O_h complex.

Remark: for the e_g SALCs we require a combination that matches the z^2 and $x^2 - y^2$ metal orbitals. Remembering that z^2 is, actually, $2z^2 - x^2 - y^2$, the former has positive lobes along the z axis that have twice the amplitude of the toroidal negative region in the xy plane. For this reason σ_1 and σ_6 are multiplied by 2.

Therefore, six group orbitals have been obtained from six ligand σ orbitals. The combination with the six central ion orbitals of the same symmetry will give rise to 12 MO: six bonding and six antibonding. The t_{2g} orbitals of the central ion (d_{xy}, d_{xz}, d_{yz}) do not have adequate symmetry and do not play a role in this type of bond. They remain, therefore, as nonbonding orbitals.

Given the above premises, the relative energy diagram of the MOs can be drawn from the relative energies of the central metal orbitals (s, p, d). Figure 1.9 shows this diagram, without taking into account any quantitative scale. The main characteristic of this diagram is that there are *always* twelve electrons in the deep bonding orbitals, as they come from the two electrons provided by each of the six ligands. Therefore, the 'important' orbitals from the point of view of the complex are the t_{2g} (nonbonding) and e_g^* (anti-bonding) orbitals. The electrons from the central ion will be placed one by one in these orbitals. We have thus arrived, albeit from a completely different angle, at the same splitting achieved with crystal field theory. The energy separation between the t_{2g} and e_g orbitals will thus be termed Δ_o. The placement of the electrons for configurations d^{4-7} will depend on the value of Δ_o. In crystal field theory this separation was a measure of the field strength; in MO theory the separation will depend upon the degree of overlap between the metal's orbitals and those of the ligand.

1.3.1.2 π Molecular Orbitals

Figure 1.10 shows schematically the ligand orbitals capable of forming π bonds. They must be perpendicular to the σ bonds. There is no unique specification of

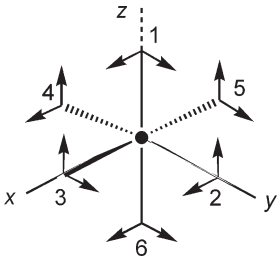

Figure 1.10 A representation of the π-ligand group orbitals (O_h symmetry).

Table 1.5 π group orbitals with their symmetry labels (O_h).

Symmetry	*Group orbitals*	*Symmetry*	*Group orbitals*
t_{1u}	$p_{2z} + p_{3z} + p_{4z} + p_{5z}$	t_{2g}	$p_{2x} + p_{3y} - p_{4x} - p_{5y}$
	$p_{1x} + p_{2x} + p_{6x} + p_{4x}$		$p_{1y} + p_{3z} - p_{6x} - p_{5x}$
	$p_{1y} + p_{3y} + p_{6y} + p_{5y}$		$p_{1x} + p_{2z} - p_{6y} - p_{4z}$
t_{1g}	$p_{2x} - p_{3y} - p_{4x} + p_{5y}$	t_{2u}	$p_{2z} - p_{3z} + p_{4z} - p_{5z}$
	$p_{1x} - p_{2z} - p_{6y} + p_{4z}$		$p_{1x} - p_{2x} + p_{6x} - p_{4x}$
	$p_{1y} - p_{3z} - p_{6x} + p_{5z}$		$p_{1y} - p_{3y} + p_{6y} - p_{5y}$

the direction of the local x and y axes, but the choice and notation in Figure 1.10 prove to be convenient in practice. It has internal consistency in that all p_x are oriented in the same x direction, all p_y in the same y direction and all p_z in the same z direction [8]. The reducible representation of these twelve ligands is $t_{2g} + t_{1u} + t_{2u} + t_{1g}$. By applying the projection operators (or simply by the same matching procedure indicated for σ orbitals) we obtain the ligand group orbitals that are able to form π bonds. The group orbitals with their symmetry labels are shown in Table 1.5.

As there are no central ion orbitals with adequate symmetry for the t_{1g} and t_{2u} group orbitals, we are left with the t_{2g} and t_{1u} group orbitals. The t_{1u} orbitals of the central ion have interacted with the other σ group orbitals of the ligands, those of the same symmetry, and thus they are not considered in this section. We are left, therefore, with the t_{2g} group orbitals, which can interact with the t_{2g} (nonbonding) orbitals of the metal ion. This π interaction is shown schematically in Figure 1.11.

The influence of these π interactions will vary according to the energy of the group orbitals (t_{2g}); these may be full p orbitals (for example, a Cl^- ion) (Figure 1.11A). As these orbitals are highly stable they will be situated further down the MO energy scale shown in Figure 1.9. In contrast, they may be high-energy empty orbitals, such as the d orbitals of a PR_3, or a π anti-bonding molecular orbital of a carbonyl group (Figure 1.11B). In this case they will be situated at the upper end of the energy scale (Figure 1.9). Figure 1.12 illustrates the energy diagram for the

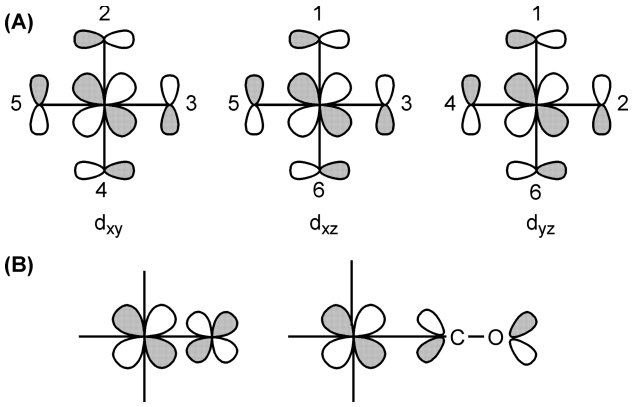

Figure 1.11 Ligand group orbitals and the corresponding metal ion orbitals, with their symmetry label (π-bond; O_h symmetry).

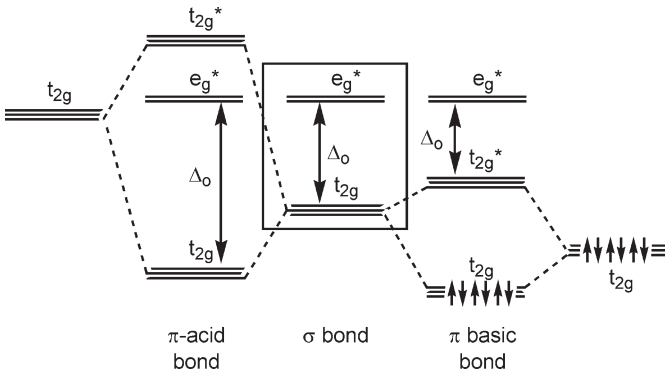

Figure 1.12 MO diagram for π-acid and π-basic ligands, in O_h geometry.

two cases. The stable ligands which are full of electrons are referred to as π-basic because, in addition to the σ(L → M) bond, they generate a π bond with the same direction: π(L → M). In contrast, the high-energy, empty ligands are known as π-acidic, as they receive electron density from the metal π(L ← M), rather than vice versa. This phenomenon is called *back donation*. It is logical to assume that for a π-basic bond to occur the metal must be highly positive, that is, have a high formal oxidation state. In contrast, π-acidic ligands serve to stabilize metal ions with high electron density, that is, with a low – or even negative – oxidation state. This is what occurs with PR_3, CO, CN^-, etc. Many organic ligands with double, triple, or delocalized bonds also fall into this category.

One of the important effects arising from the contribution of the two types of π bond is the variation produced in the Δ_o value (Figure 1.12). The π-basic ligands

reduce the value of this parameter. Therefore, the first ligands of the spectrochemical series are those which produce this type of interaction: the halides. In contrast, PR_3, CO, CN^-, etc. come at the end of the spectrochemical series as they yield a very high value of Δ_o, due to their being π-acidic ligands.

1.3.2
Molecular Orbitals of a Tetrahedral Complex

The steps to be followed here are the same as in the case of octahedral complexes. They must first be carried out for σ interactions and then for π interactions. In the T_d point group the four σ orbitals of the ligands can be grouped according to the group orbitals $a_1 + t_2$ (Figure 1.13). This can be verified by means of group theory. By applying the corresponding projection operators we obtain the group orbitals as linear combinations of these four orbitals, and their adaptation to the symmetry of the central ion orbitals can be correlated. This result is shown in Table 1.6 (the numbering refers to that used in Figure 1.13).

In Figure 1.13 only the s and p orbitals of the central ion are taken into account, but it should be remembered that the d_{xy}, d_{xz} and d_{yz} orbitals have the same symmetry (t_2) as the three p orbitals. Thus, there will always be a mixture of both types of orbital. Bearing this important point in mind, the corresponding energy diagram for the molecular orbitals obtained is shown schematically in Figure 1.14.

For π-group orbitals, although this is not immediately obvious due to their orientation, these orbitals belong to the symmetry species $t_1 + t_2 + e$. The t_1 group orbitals do not correspond to any central ion orbital and the t_2 group form σ bonds. The orientation and the MOs with e symmetry, as well the energy diagram including the σ and π bonds, are difficult to visualize due to the presence of mixed orbitals. For a complete study see Ref. [2].

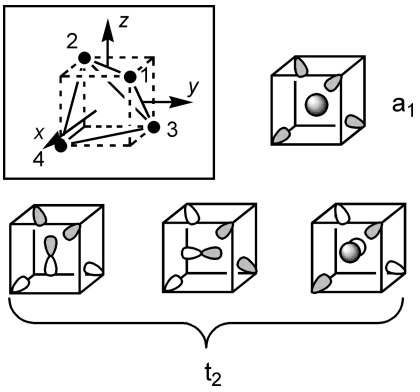

Figure 1.13 Ligand group orbitals and the corresponding metal ion orbitals, with their symmetry label (σ-bond; T_d symmetry).

Table 1.6 σ group orbitals for T_d symmetry.

Symmetry	*Metal orbitals*	*Group orbitals*
a_1	s	$\sigma_1 + \sigma_2 + \sigma_3 + \sigma_4$
t_2	(p_x, p_y, p_z)	$\sigma_1 + \sigma_2 - \sigma_3 - \sigma_4$
	(d_{xy}, d_{xz}, d_{yz})	$\sigma_1 - \sigma_2 - \sigma_3 + \sigma_4$
		$\sigma_1 - \sigma_2 + \sigma_3 - \sigma_4$

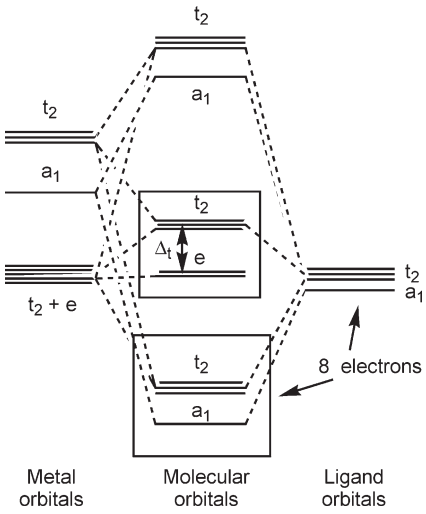

Figure 1.14 MO diagram (only σ orbitals) for a T_d complex.

1.3.3 Molecular Orbitals of a Square-planar Complex

In the D_{4h} point group the four σ orbitals of the ligands can be grouped according to the group orbitals $a_{1g} + e_u + b_{1g}$. This can be verified by means of group theory. By applying the corresponding projection operators we obtain the group orbitals as linear combinations of these four orbitals, and their adaptation to the symmetry of the central ion orbitals can be correlated. This result is shown in Table 1.7 and Figure 1.15.

There are two kinds of π group orbitals: those in the molecular plane and those which are perpendicular to it (Figure 1.16). The first four belong to the symmetry species $a_{2g} + e_u + b_{2g}$, while the four perpendicular ones belong to the species $a_{2u} + e_g + b_{2u}$. By applying the corresponding projection operators we obtain the group orbitals as linear combinations of these eight orbitals, and their adaptation to the symmetry of the central ion orbitals can be correlated. This result is shown in Table 1.8 and Figure 1.16A for b_{2g} and e_u π orbitals. The corresponding π_z MO orbitals can be easily deduced by the reader following an analogous procedure.

Table 1.7 σ group orbitals for D_{4h} orbitals.

Symmetry	*Metal orbitals*	*Group orbitals*
a_{1g}	s, d_{z2}	$\sigma_1 + \sigma_2 + \sigma_3 + \sigma_4$
e_u	(p_x, p_y)	$\sigma_1 + \sigma_2 - \sigma_3 - \sigma_4$
		$-\sigma_1 + \sigma_2 + \sigma_3 - \sigma_4$
b_{1g}	d_{x2-y2}	$\sigma_1 - \sigma_2 + \sigma_3 - \sigma_4$

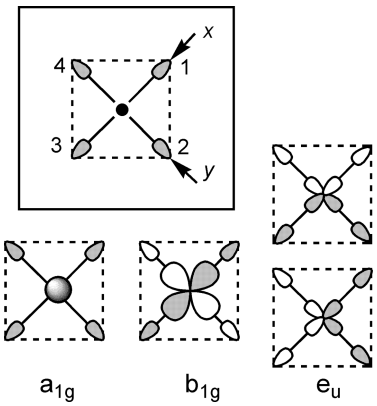

Figure 1.15 Ligand group orbitals and the corresponding metal ion orbitals, with their symmetry label (σ-bond; square planar geometry).

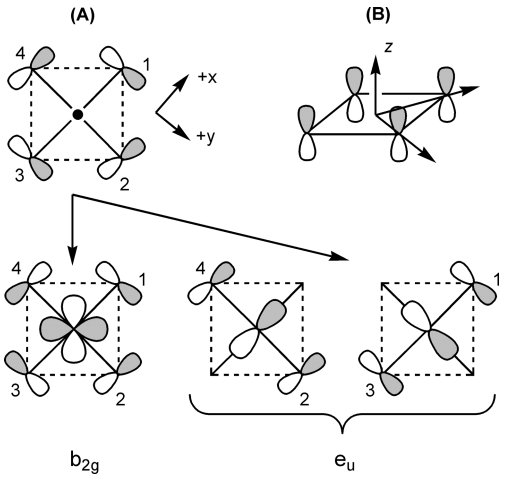

Figure 1.16 Ligand group orbitals and the corresponding metal ion orbitals, with their symmetry label (π-bond; square planar geometry).

Table 1.8 π group orbitals for D_{4h} geometry (the numbering is that used in Figure 1.16).

Symmetry	*Metal orbitals*	*Group orbitals*
a_{2u}	p_z	$p_{1z} + p_{2z} + p_{3z} + p_{4z}$
e_g	(d_{xy}, d_{xz})	$p_{1z} - p_{3z}$; $p_{2z} - p_{4z}$
b_{2u}	–	$p_{1z} - p_{2z} + p_{3z} - p_{4z}$
a_{2g}	–	$p_{1y} - p_{2x} - p_{3y} + p_{4x}$
e_u	(p_x, p_y)	$p_{2x} + p_{4x}$; $p_{1y} + p_{3y}$
b_{2g}	d_{xy}	$p_{1y} + p_{2x} - p_{3y} - p_{4y}$

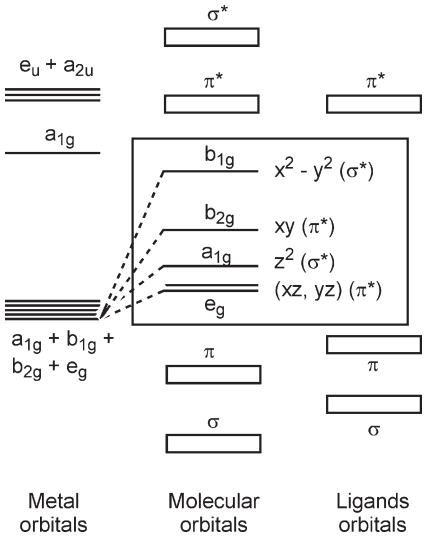

Figure 1.17 Schematic MO diagram for a complex with square-planar geometry.

The corresponding – and simplified – energy diagram for the MO obtained is shown schematically in Figure 1.17. The ordering of energies will be discussed in Section 1.4.4.

1.3.4
Mixed Ligands and Other Geometries

The reader interested in octahedral complexes with one carbonyl (π-acidic) ligand and one π-basic ligand as well as in more complicated complexes, such as $[MCl_2L_4]$, $[MCl_3L_3]$, $[M(CO)_2L_4]$, $[M(CO)_3L_3]$ may consult the excellent treatment given by Y. Jean in his book [6].

For other geometries, such as square-pyramidal, trigonal bipyramidal (ML_5), trigonal-planar (ML_3), "butterfly" (ML_4), linear or angular ML_2 complexes, and their relationships, the reader may also consult the same book [6].

1.3.5 Nobel Prizewinning Discoveries of Complexes

1.3.5.1 Metallocenes

The discovery of the remarkably stable organometallic compound ferrocene $[Fe(\eta^5\text{–}C_5H_5)_2]$ occurred in 1951. Two research workers, Ernst-Otto Fisher in Munich and Geoffrey Wilkinson in London, were awarded the Nobel Prize in 1973 for their contributions.

The discussion of the bonding does not depend critically on whether the preferred rotational orientation of the two rings is staggered (D_{5d}) or eclipsed (D_{5h}); in any event, the barriers to ring rotation in all types of arene-metal complexes are very low, ca. 10–20 kJ mol^{-1}. Applying group theory and looking at the number of nodal planes, it is easy to demonstrate that the shapes and relative energies of the five π-orbitals in an isolated $C_5H_5^-$ are as shown in Figure 1.18 ($C_5H_5^-$ has 6 electrons). Considering, now, the two rings together and assuming D_{5d} symmetry, the representation of the 10 π-orbitals is given in Table 1.9. The reduction for the representation Γ_π gives: $a_{1g} + a_{2u} + e_{1g} + e_{1u} + e_{2g} + e_{2u}$.

Considering the symmetry labels (and energies) of the iron(II) orbitals, and combining them with the group orbitals of the two Cp ligands, an approximate MO diagram for ferrocene is shown in Figure 1.19. The principal bonding interac-

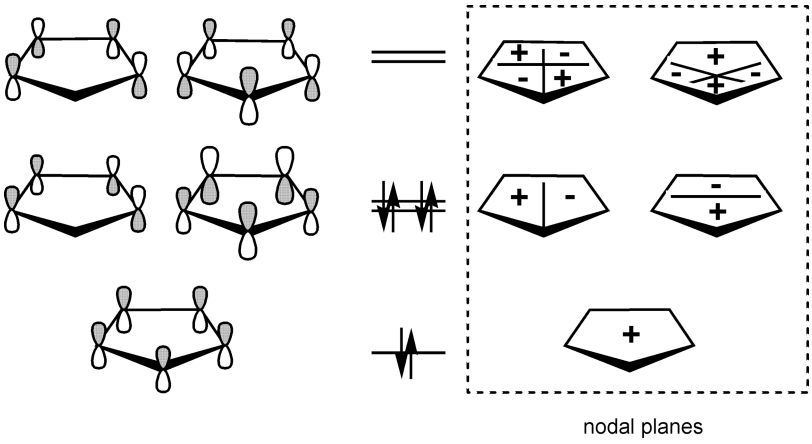

Figure 1.18 MOs for a $C_5H_5^-$ ring.

Table 1.9 Reducible representation of the 10 π-orbitals.

D_{5d}	E	$2C_5$	$2C_5^2$	$5C_2$	i	$2S_{10}$	$2S_{10}^3$	$5\sigma_d$
Γ_π	10	0	0	0	0	0	0	2

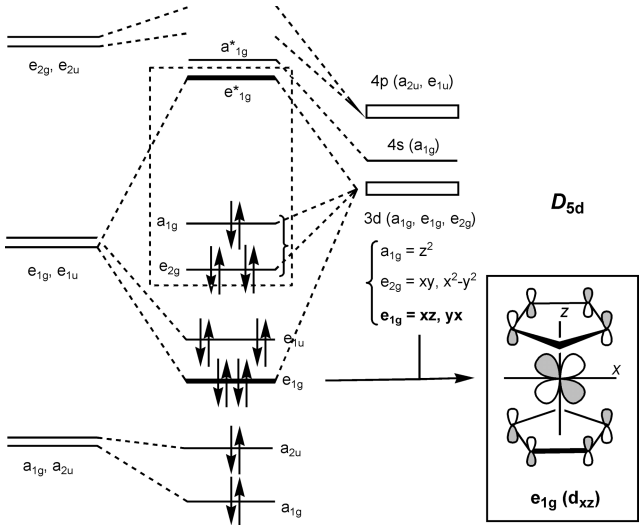

Figure 1.19 Scheme of the MOs in the ferrocene structure.

tion is that giving rise to the strongly bonding e_{1g} and strongly antibonding e_{1g}^* orbitals. To give one concrete example of how ring and metal orbitals overlap, the nature of this particular important interaction is illustrated in Figure 1.19 (inset). The other d orbitals (z^2, $x^2 - y^2$, and xy) make up a block of three nonbonding or nearly nonbonding orbitals. In fact, $x^2 - y^2$ and xy (e_{2g}) are stabilized by bonding interactions with the π^* orbitals of appropriate symmetry on the Cp rings. The order given in this figure may be different to that found in other books, mainly for the antibonding MOs. The metal orbitals e_{2g} and a_{1g} can be reversed, depending on the metal and the type of calculation.

1.3.5.2 Carbenes

Three chemists were awarded the Nobel Prize in 2005, "*for the development of the metathesis method in organic synthesis*": Y. Chauvin, R. H. Grubbs and R. R. Schrock. Two of them (Grubbs and Schrock), have developed catalysts that improve considerably the metathesis effect. These catalysts are metal-carbene derivatives [9, 10]. Carbene complexes, whose general formula is $[L_nM{=}CR_2]$ formally contain an M=C double bond. Two group orbitals can be constructed for the bond with the metal center: a hybrid, sp and a pure orbital, p (Figure 1.20A).

There are two limiting cases: *Fisher carbenes* and *Schrock carbenes*. If we consider the carbene as an L-type ligand (with two electrons in the s type orbital) it therefore acts as a σ donor, which interacts with an empty orbital of the metal (e.g. z^2). In this model the p orbital is empty, so the carbene acquires a π-acceptor character (Figure 1.20A). This orbital can be either higher or lower in energy than the d orbitals on the metal.

When the p orbital is higher in energy than the d orbital, we obtain a typical back-donation scheme with the formation of a bonding MO mainly located on the

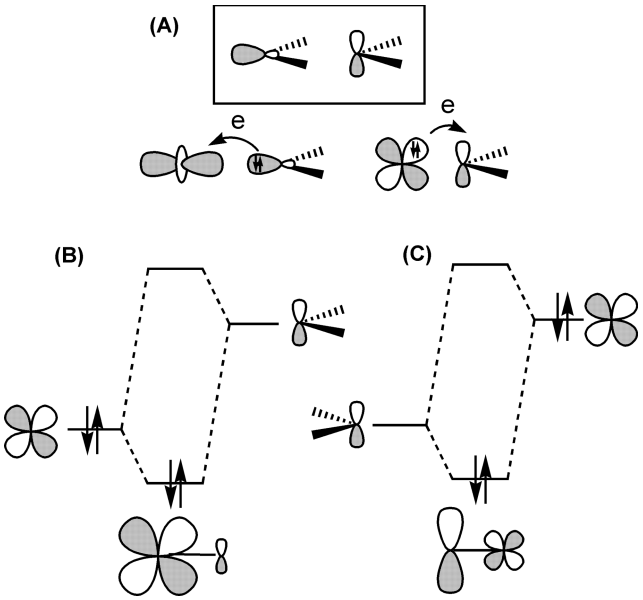

Figure 1.20 HOMO and LUMO in carbene complexes (see text for explanation).

metal (Figure 1.20B). However, if the p orbital is lower in energy than the d orbital, the occupied bonding MO is mainly concentrated on the carbene so that, in a formal sense, two electrons have been transferred from the metal to this ligand (Figure 1.20C), which leads to an 'increase' in the metal's oxidation state by two units.

The first situation (Figure 1.20B) is found for metals with d orbitals low in energy (right-hand side of the periodic table). In addition the presence of π-acceptor ligands also leads to a lowering of the level of the d orbitals. As far as the carbene is concerned, the energy of the p orbital is raised if the substituents are π-donors, that is, they have lone pairs (halogens, OR, NR_2, etc.). Carbene complexes that possess these characteristics are called *Fischer carbenes*. $[(CO)_5W{=}C(Ph)(OMe)]$ and $[Cp(CO)(PPh_3)Fe{=}CF_2]^+$ are paradigmatic examples. These carbenes are [M(δ–)=C(δ+)], with an electrophilic character for the carbon center.

The second situation (Figure 1.20C) is found for metals on the left-hand side of the periodic table, and must have π-donor ligands to destabilize the d orbital. Moreover, to ensure that the p orbital on the carbene is as low in energy as possible, its substituents cannot be π donor: CH_2 is itself a good candidate and, more generally, alkyl substituents are suitable (the term 'alkylidene' is often used for a carbene substituted by alkyl groups). Two examples are $[Cp_2(CH_3)Ta{=}CH_2]$ and $[CpCl_2Ta{=}C(H)(CMe_3)]$. The metal in this group of complexes is usually considered to be oxidized by two units by the alkylidene ligand, so the two examples mentioned above contain Ta(V). These carbenes are called *Schrock carbenes*. Now the electron polarization is [M(δ+)=C(δ–)].

1.4
Angular Overlap Model [11]

The angular overlap model is a simple and quantitative method that enables the energy of the molecular orbitals to be calculated from certain pre-established simplifications and tables. It is based on the quantum consideration that an orbital, described in polar coordinates, has a radial part and an angular part: $\Phi = R(r) \cdot Y(\theta,\phi)$ (Figure 1.1). The expressions of Φ for the d orbitals are shown in Table 1.1.

1.4.1
Overlap Integral

From the two orbitals μ and ν we can derive what is known as the overlap integral, given by: $S_{\mu\nu} = <\phi_\mu|\phi_\nu> = S'_{\mu\nu}(\lambda, r) \cdot S''_{\mu\nu}(\lambda, \theta, \phi)$. λ depends on the type of atomic orbital, which may be σ, π or δ molecular orbitals.

A simple example to study is the typical case of angular dependence in the overlap between two orbitals: an s orbital that rotates around a d_{z2} orbital, modifying the overlap angle (Figure 1.21). The overlap will be proportional to $3\cos^2\theta - 1$ (Table 1.1), and is shown graphically in Figure 1.21. It can be seen that for an angle θ of 54.73° the overlap S is zero.

1.4.2
Energy of the Molecular Orbitals

The interaction energy associated with two atomic orbitals that overlap to form a molecular orbital is: $E_{\mu\nu} = <\phi_\mu |\hat{H}| \phi_\nu>$. The energy is negative (stabilization of the MO formed) when the overlap is positive, and positive (destabilization of the MO formed) when the overlap is negative. The *angular overlap model* is the simplest way of calculating the energies of the MO as it only considers the angular part of the wavefunction. The value of the stabilization (or destabilization) energy is $E \approx S_{ij}^2$. The model is only useful for comparisons and relative calculations, and not for absolute calculations.

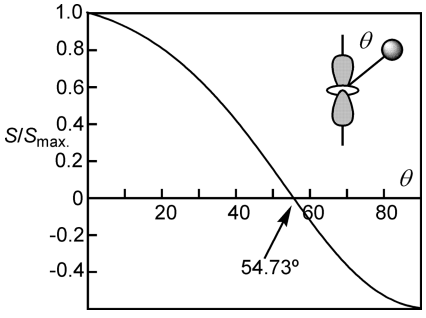

Figure 1.21 Variation of the relative overlap (S/S_{max}) varying the θ angle (see text).

1.4.3
The Additive Character Rule

When an atomic orbital of a metal overlaps with several atomic orbitals of ligands, the relative calculation of the stabilization (or destabilization) energy is given by what is termed the *additivity rule:* $E \approx \Sigma_n S_\lambda^2$ (n = ligand; $\lambda = \sigma, \pi, \delta$).

As we are interested in coordination complexes the sign given to the energy value must be taken into account. In general, the sign of the angular overlap parameter is given by the donor or acceptor nature of the ligands with respect to the central atom (transition ion). Although the σ bonds are always donors, this is not the case for the π bonds. For donor ligands the sign will be positive (destabilization of the MO, as we are considering anti-bonding orbitals). When the ligands are acceptors (π-acids) the sign is negative (stabilization of the anti-bonding molecular orbital), but *always* after considering the σ contribution, which is anti-bonding.

1.4.4
Tables for Calculating the Angular Overlap Parameters

Table 1.10 gives the general expressions for the relative values of S, with respect to θ and ϕ, for various types of overlap involving a central transition ion and the s and p orbitals of the ligands.

This general table can be used to construct other simplified tables which give the values of E_σ and E_π for the complexes with the commonest geometry directly. For example, Figure 1.22 shows the positions of various ligands, which readily enables the parameters E_σ and E_π to be calculated for the most usual geometries. These parameters are given directly in Table 1.11, as energy values proportional to S^2.

Table 1.10 Angular dependence of overlap integrals (for the s and p orbitals of the ligands with regard to the d orbital of the central ion).

S	*Expression*	S	*Expression*
s, z^2	$(3H^2 - 1)S_\sigma/2$	x, z^2	$\sqrt{3}FH^2S_\pi + F(3H^2 - 1)S_\sigma/2$
s, xz	$\sqrt{3}\ FHS_\sigma$	x, xz	$-H(1 - 2F^2)S_\pi + \sqrt{3}F^2\mathrm{H}S_\sigma$
s, yz	$\sqrt{3}\ GHS_\sigma$	x, yz	$FGH(\sqrt{3}S_\sigma + 2S_\pi)$
s, xy	$\sqrt{3}\ FGS_\sigma$	x, xy	$-G(1 - 2F^2)S_\pi + \sqrt{3}F^2GS_\sigma$
s, $x^2 - y^2$	$\sqrt{3}\ (F^2 - G^2)S_\sigma/2$	x, $x^2 - y^2$	$-F(1 - F^2 + G^2)S_\pi + \sqrt{3}F(F^2 - G^2)S_\sigma/2$
z, z^2	$-\sqrt{3}H(1 - H^2)S_\pi + H(3H^2 - 1)S_\sigma/2$	y, z^2	$\sqrt{3}\ GH^2S_\pi + G(3H^2 - 1)S_\sigma/2$
z, xz	$-F(1 - 2H^2)S_\pi + \sqrt{3}\ FH^2S_\sigma$	y, xz	$FGH(\sqrt{3}S_\sigma + 2S_\pi)$
z, yz	$-G(1 - 2H^2)S_\pi + \sqrt{3}\ GH^2S_\sigma$	y, yz	$-H(1 - 2G^2)S_\pi + \sqrt{3}G^2HS_\sigma$
z, xy	$FGH(\sqrt{3}S_\sigma + 2S_\pi)$	y, xy	$-F(1 - 2G^2)S_\pi + \sqrt{3}\ FG^2S_\sigma$
z, $x^2 - y^2$	$-H(G^2 - F^2)S_\pi + \sqrt{3}H\ (F^2 - G^2)S_\sigma/2$	y, $x^2 - y^2$	$-G(G^2 - F^2 - 1)S_\pi + \sqrt{3}G(F^2 - G^2)S_\sigma/2$

$F = \sin\theta\cos\phi$; $G = \sin\theta\sin\phi$; $H = \cos\theta$.

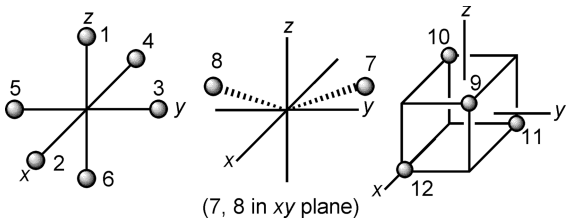

Figure 1.22 Fixed position for ligands in several common geometries.

Table 1.11 Angular proportionality factors for E_σ and E_π. The numbering (1–12) corresponds to that used in Figure 1.22.

Position of the ligand	z^2	$x^2 - y^2$	xz	yz	xy
1 σ	1	0	0	0	0
π	0	0	1	1	0
2 σ	1/4	3/4	0	0	0
π	0	0	1	0	1
3 σ	1/4	3/4	0	0	0
π	0	0	0	1	1
4 σ	1/4	3/4	0	0	0
π	0	0	1	0	1
5 σ	1/4	3/4	0	0	0
π	0	0	0	1	1
6 σ	1	0	0	0	0
π	0	0	1	1	0
7 σ	1/4	3/16	0	0	9/16
π	0	3/4	1/4	3/4	1/4
8 σ	1/4	3/16	0	0	9/16
π	0	3/4	1/4	3/4	1/4
9 σ	0	0	1/3	1/3	1/3
π	2/3	2/3	2/9	2/9	2/9
10 σ	0	0	1/3	1/3	1/3
π	2/3	2/3	2/9	2/9	2/9
11 σ	0	0	1/3	1/3	1/3
π	2/3	2/3	2/9	2/9	2/9
12 σ	0	0	1/3	1/3	1/3
π	2/3	2/3	2/9	2/9	2/9

Another way of presenting these tables is to consider the various geometries with the sum of the contribution of each ligand, calculated previously. This offers a much quicker way of comparing the stability of the molecular orbitals formed for each geometry. The most noteworthy cases are shown in Table 1.12.

Table 1.12 σ and π interaction energy for various geometries.

Geometry	z^2		$x^2 - y^2$		xy		xz		yz	
	σ	π	σ	π	σ	π	σ	π	σ	π
MY linear, $C_{\infty v}$	1	0	0	0	0	0	0	1	0	1
MY_2 linear, $D_{\infty h}$	2	0	0	0	0	0	0	2	0	2
angular, C_{2v}	1/2	0	3/2	0	0	2	0	1	0	1
MY_3 facial trivacant, C_{3v}	3/2	0	3/2	0	0	2	0	2	0	2
triangular, D_{3h}	3/4	0	9/8	3/2	9/8	3/2	0	3/2	0	3/2
T form, C_{2v}	3/2	0	3/2	0	0	2	0	1	0	3
MY_4 tetrahedron, T_d	0	8/3	0	8/3	4/3	8/9	4/3	8/9	4/3	8/9
square-planar, D_{4h}	1	0	3	0	0	4	0	2	0	2
trigonal pyramid, C_{3v}	7/4	0	9/8	3/2	9/8	3/2	0	5/2	0	5/2
cis-divacant, C_{2v}	5/2	0	3/2	0	0	2	0	3	0	3
MY_5 trigonal bipyramid, D_{3h}	11/4	0	9/8	3/2	9/8	3/2	0	7/2	0	7/2
square pyramid, C_{4v}	2	0	3	0	0	4	0	3	0	3
MY_6 octahedron, O_h	3	0	3	0	0	4	0	4	0	4
trigonal prism, D_{3h}	3/8	0	9/16	3/2	9/16	3/2	2.25	1.5	2.25	1.5
MY_7 pentagonal bipyramid, D_{5h}	13/4	0	15/8	5/2	15/8	5/2	0	9/2	0	9/2
MY_8 cube, O_h	0	16/3	0	16/3	8/3	16/9	8/3	16/9	8/3	16/9
square antiprism, D_{4d}	0	2/3	4/3	32/9	4/3	32/9	8/3	37/9	8/3	37/9
MY_{12} icosahedron, I_h	12/5	24/5	12/5	24/5	12/5	24/5	12/5	24/5	12/5	24/5

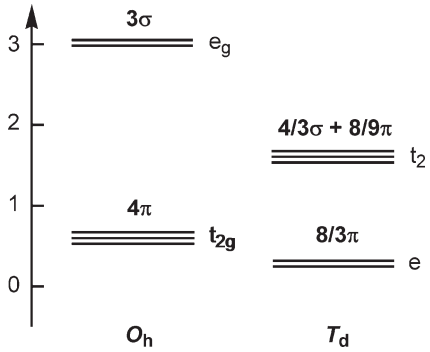

Figure 1.23 Energy calculation from the overlap angular model for O_h and T_d complexes.

1.4.5
Examples of Use of the Above Tables

The relative energies of the MO of octahedral and tetrahedral complexes can be easily deduced by using Tables 1.11 and 1.12, and the results of this are shown schematically in Figure 1.23. The quotient $\Delta S_{tet}/\Delta S_{oct}$ gives the value 4/9, as pointed out above.

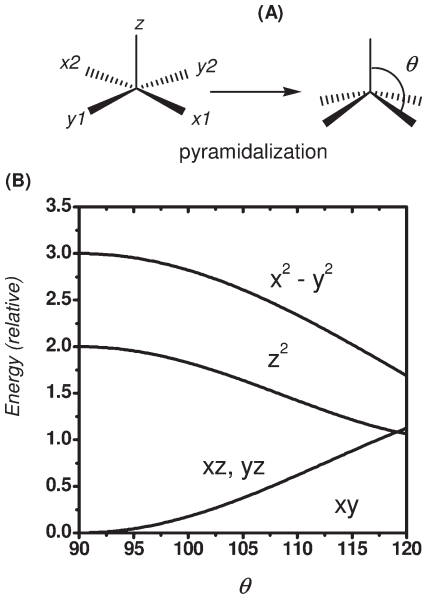

Figure 1.24 Walsh diagram for the pyramidalization of a square-pyramidal geometry.

Table 1.13 $E(\sigma) = \Sigma S_\sigma^2$ of the four equatorial orbitals in a square-base pyramid complex.

	S/S_σ	S^2/S_σ^2	S^2/S_σ^2	ϕ	S^2/S_σ^2
s, $x^2 - y^2$	$\sqrt{3}/(F^2 - G^2)/2$	$3/4(F^2 - G^2)^2$	$3/4(\sin^2\theta \cos^2\phi - \sin^2\theta \sin^2\phi)^2$	0	$3/4(\sin^2\theta)^2$
				90	id
				180	id
				270	id
s, z^2	$(3H^2 - 1)/2$	$1/4(3H^2 - 1)^2$	$1/4(3\cos^2\theta - 1)^2$	–	$1/4(3\cos^2\theta - 1)^2$
s, xz	$\sqrt{3}FH$	$3F^2H^2$	$3\sin^2\theta \cos^2\phi \cos^2\theta$	0	$3\sin^2\theta \cos^2\theta$
				90	0
				180	$3\sin^2\theta \cos^2\theta$
				270	0
s, yz	$\sqrt{3}GH$	$3G^2H^2$	$3\sin^2\theta \sin^2\phi \cos^2\theta$	0	0
				90	$3\sin^2\theta \cos^2\theta$
				180	0
				270	$3\sin^2\theta \cos^2\theta$
s, xy	$\sqrt{3}FG$	$3F^2G^2$	$3\sin^2\theta \cos^2\phi \sin^2\theta \sin^2\phi$	0	0
				90	0
				180	0
				270	0

Starting from Table 1.10 it is easy to construct the Walsh diagram for the pyramidalization of a square-base pyramid complex, which is a common occurrence in this type of complex. The phenomenon of pyramidalization is shown schematically in Figure 1.24A. If we restrict our attention to the σ bonds of the four equatorial orbitals the functions that must be represented are $E(\sigma) \approx \Sigma S_\sigma^2$ (Table 1.13).

Therefore, the final values, summing the four values for the four ϕ angles, are: $x^2 - y^2 = 3(\sin^2\theta)^2$; xz, $yz = 6\sin^2\theta\cos^2\theta$; $xy = 0$; $z^2 = (3\cos^2\theta - 1)^2$. To these values must be added the overlap σ with the ligand in the apical position, which is invariant when pyramidalized and has a maximum value of $S/S_\sigma = 1$ for the z^2 orbital and 0 for the remaining cases. The representation of these trigonometric functions for angles from 90° (non-pyramidalization) to 120° gives the Walsh diagram shown in Figure 1.24B.

References

1 Figgis, B.N., Hitchman, M.A. (2000) *Ligand Field Theory and its Applications*, Wiley-VCH, Weinheim.

2 Cotton, F.A. (1990) *Chemical Applications of Group Theory*, 3rd edn., John Wiley & Sons, New York.

3 Jorgenssen, C.K. (1971) *Modern Aspects of Ligand Field Theory*, Elsevier, New York.

4 Huheey, J.A., Keiter, E.A., Keiter, R.L. (1993) *Inorganic Chemistry: Principles of Structure and Reactivity*, 4th edn., Harper Collins, New York.

5 Tudela, D., A Common Inorganic Chemistry Textbook Mistake: Incorrect Use of Pairing Energy in Crystal Field Stabilization Energy Expressions, *J. Chem. Educ.* 1999, *76*, 134.

6 Jean, Y. (2005) *Molecular Orbitals of Transition Metal Complexes*, Oxford University Press, Oxford.

7 C.A.C.A.O: Package of Programs for Molecular Orbital Analysis, Mealli, C., Proserpio, D.M. MO Theory made visible (CS), *J. Chem. Educ.* 1990, *67*, 399.

8 Kettle, S.F.A. (1992) *Symmetry and Structure*, John Wiley & Sons, Chichester.

9 (a) Schrock, R.R., Murdzek, J.S., Bazan, G.C., Robbins, J. , DiMare, M., O'Regan, M., Synthesis of molybdenum imido alkylidene complexes and some reactions involving acyclic olefins, *J. Am. Chem. Soc.* 1990, *112*, 3875–3886; (b) Bazan, G.C., Oskam, J.H., Cho, H.-N., Park, L.Y., Schrock, R.R., Living ring-opening metathesis polymerization of 2,3-difunctionalized 7-oxanorbornenes and 7-oxanorbornadienes by $Mo(CHCMe_2R)(NC_6H_3\text{-iso-}Pr_2\text{-}2,6)(O\text{-}tert\text{-}Bu)_2$ and $Mo(CHCMe_2R)(NC6H_3\text{-iso-}Pr_2\text{-}2,6)(OCMe_2CF_3)_2$, *J. Am. Chem. Soc.* 1991, *113*, 6899–6907.

10 (a) Nguyen, S.T., Johnson, L.K., Grubbs, R.H., Ring-opening metathesis polymerization (ROMP) of norbornene by a Group VIII carbene complex in protic media, *J. Am. Chem. Soc.* 1992, *114*, 3974; (b) Wu, W., Nguyen, S.T., Grubbs, R.H., Ziller, J.W., Reactions of Ruthenium Carbenes of the Type $(PPh_3)_2(X)_2Ru{=}CH{-}CH{=}CPh_2$ (X=Cl and CF_3COO) with Strained Acyclic Olefins and Functionalized Olefins, *J. Am. Chem. Soc.* 1995, *117*, 5503–5511.

11 (a) Burdett, J.K., A new look at structure and bonding in transition metal complexes. *Adv. Inorg. Chem.* 1978, *21*, 113; (b) Hoggard, P.E., Angular overlap model parameters, *Struct. Bond.*, 2004, *106*, 37. See the explanation given in, Purcell, K.F., Kotz, J.C. (1979) *Inorganic Chemistry*, Saunders Company, Philadelphia.